



Australian Government

Department of Agriculture, Fisheries and Forestry

# Technical Report

**Program and KPI:** Sub-program 1.2 KPI 3.12

**Report Title:** DEXA prediction of lean beef trim

**Prepared by:** Ben Madlener, Honor Calnan and Graham Gardner  
Murdoch University

**Date published:** 30 September 2021



## **Citation**

Madlener, B., Calnan H.B., Gardner G.E. (2021). Dual energy X-ray Absorptiometry (DEXA) prediction of lean trim. An *Advanced measurement technologies for globally competitive Australian meat* Project. September.

## **Acknowledgements**

This project was coordinated through the Advanced Livestock Measurement Technologies Project (ALMTech) and funded by the Department of Agriculture Rural Research and Development (R&D) for Profit program and Meat and Livestock Australia. The authors gratefully acknowledge the contribution of the staff and resources at Teys Australia and Texas Technical University in data collection and the staff at Murdoch University for their support in image acquisition and data analysis.

## Abstract

This experiment assessed the ability of a commercial-prototype dual energy x-ray absorptiometer (DEXA) to predict the composition of beef sides scanned at abattoir line-speed and thereby determine the lean trim weights from each beef carcass side. It was hypothesised that DEXA provided a better objective measure of whole carcass composition than the current industry standard of P8 fatness, and therefore, would predict lean trim weights with higher precision and accuracy than P8 fatness. 250 beef carcasses representing a wide range in carcass weight and fatness (measured by P8 fat depth) were selected for DEXA scanning and a comprehensive bone-out into retail cuts of meat and trim. Boners assigned lean trim to one of three categories: 60, 85 or 90% chemical lean (CL), based on the visual fatness of the trim according to standard processor protocols. The weight of this trim was predicted in general linear models using hot side weight (HSW) and P8 fatness or DEXA variables as covariates. To address the anticipated difficulty boners faced in visually differentiating 85 and 90% CL, we also used the above models to predict summed 85 and 90% CL trim. In line with our hypothesis, DEXA variables predicted beef trim weights with better precision than P8 fatness, though the differences were small. The precision of prediction varied between trim categories. In the fatter trim category (65% CL), DEXA variables predicted the weight of trim with less precision, with an R-squared of 0.78 and a root mean square error of prediction (RMSEP) of 106 grams. In contrast, precision was improved when predicting the weight of the combined leaner trim category (85+90% CL), with an R-squared value of 0.92 and an RMSEP of 60 grams. The DEXA system differentiated a greater range in trim weight than P8 fatness and therefore has potential as a novel technology to predict beef trim weights in a commercial setting.

# Contents

Citation .....	2
Acknowledgements.....	2
Abstract.....	3
Contents .....	4
1 Introduction .....	5
2 Materials and methods.....	6
2.1 Carcase selection and slaughter protocol .....	6
2.2 DEXA image acquisition.....	6
2.3 Bone-out protocol and lean trim measurement.....	7
2.4 DEXA image analysis .....	7
2.5 Statistical Analysis .....	9
3 Results.....	11
4 Discussion .....	17
4.1 Precision and accuracy of DEXA prediction of trim weights .....	17
4.2 Industry implications and future work .....	19
5 Conclusions .....	20
6 References .....	20

# 1 Introduction

The weight of saleable meat in a carcass is a key profit driver across the entire beef supply chain. Most of the saleable beef sourced from each carcass is found in the mass of the commercial cuts. However, the fabrication of cuts to market specifications relies on trimming excess tissue, resulting in a saleable trimmed by-product containing both lean meat and fat. Predicting the weight of trim procured from beef carcasses prior to manufacturing is valuable to processors (Gardner et al., 2021; Hocking Edwards et al., 2015). Firstly, carcasses of the same weight can be cut up in multiple ways to procure a variety of commercial cuts. Providing processors with the capacity to predict the weight of commercial cuts prior to fabrication enables them to accurately allocate carcasses on hand into cutting plans for certain markets, maximising profit and minimising waste. The weight of trimmed meat is a component of this value and therefore inclusion of trim in pre-fabrication predictions will improve the accuracy of these sorting decisions. Secondly, as trimmed meat is a valuable commodity, forecasting the likely amount produced will improve the responsiveness of later steps in the supply chain wherein markets for this product are sought. Finally, benchmarking of staff performance is used by processors to improve boning room efficiency, thus predicting the weight of saleable meat, including commercial cuts and lean trim, is essential to enable accurate performance benchmarking.

Carcasses of equal weight can produce substantially different cut and trim weights depending on their composition i.e., the proportions of lean meat, fat and bone of the carcass. Fatter carcasses yield relatively smaller saleable cuts, a greater proportion of fatty trim and require more time to trim to specification, reducing boning room efficiency. In recent years the Australian beef industry has invested in the development of objective technologies that aim to improve measurement of carcass composition, and thereby improve our ability to predict the quantity of lean trim procured from the carcass. The current beef industry standard for estimating carcass composition is to take a single point measurement of carcass fat depth at the P8 site (Johnston et al., 2003) or fat depth over the rib quartering site (Watson et al., 2008). However, these single point measures of fatness have been demonstrated to poorly predict beef carcass composition (Williams et al., 2017). Given that lean trim weight and composition are likely associated with whole carcass composition, single point measures of fatness are anticipated to also predict trim characteristics poorly. Thus, current research and development is focused on technologies capable of measuring whole carcass composition.

Dual Energy X-Ray Absorptiometry (DEXA) is one technology capable of measuring whole carcass composition, and therefore may be capable of improving the prediction of lean trim weight procured from carcasses. A DEXA system capable of rapid imaging, and thereby of operating in an abattoir environment, has recently been developed to precisely and accurately predict the carcass composition (Gardner et al., 2018) and thereby cut weights (Gardner et al., 2021) of lamb carcasses scanned at abattoir chain speed. This prototype DEXA system has also been shown to have a high degree of precision and accuracy when predicting the composition of beef carcasses (Calnan et al., 2021; Gardner et al., 2017), leading to the installation of the first commercial beef DEXA system.

This study assessed the capacity of a commercial beef DEXA system to predict the weight of lean trim produced from beef sides scanned at abattoir line speed. We hypothesise that the

DEXA system will predict beef trim weights with higher precision and accuracy than predictions made using P8 fat depth.

## 2 Materials and methods

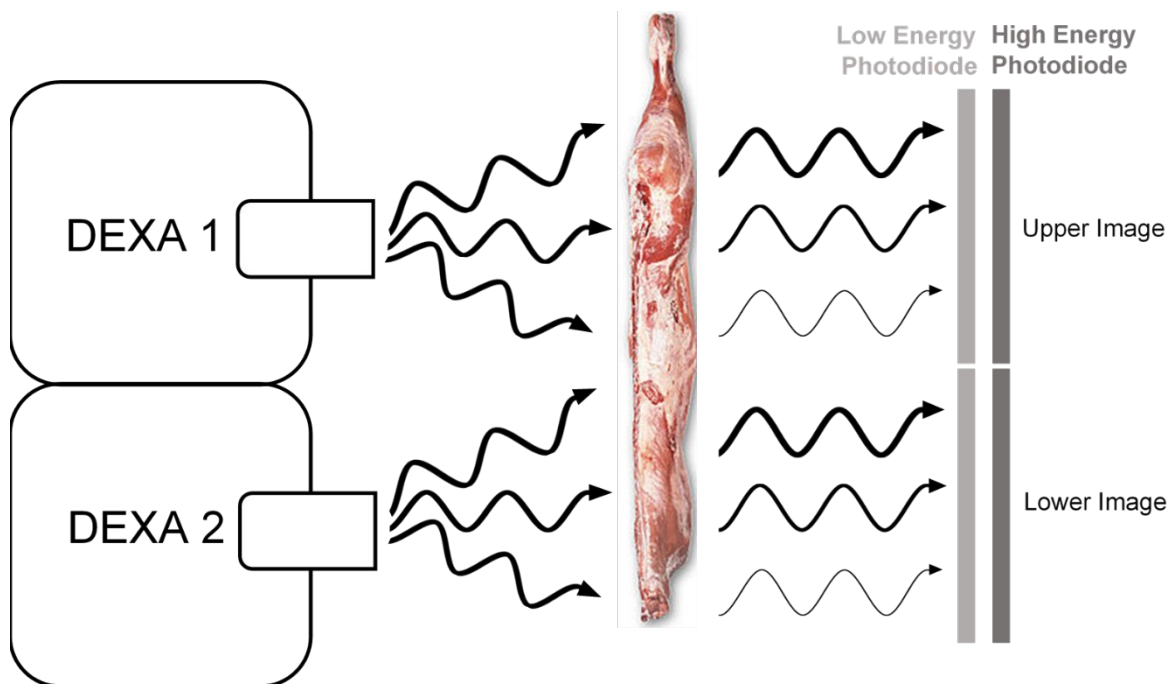
### 2.1 Carcase selection and slaughter protocol

Data was collected at Teys Lakes Creek abattoir in Rockhampton QLD. 263 *Bos indicus* cross bred beef sides were selected over a 21-day production period. Following slaughter, the heifer and steer (up to 4 tooth) carcasses were split into sides, weighed (hot side weight or HSW) and measured for P8 fat depth. The sides were selected on the slaughter floor based on HSW and P8 fat depth to represent a wide range in carcase weight and fatness (Table 1), before undergoing standard chilling protocols.

### 2.2 DEXA image acquisition

Each day of the experiment following initial selection, 10 to 14 beef sides were taken from the chiller for DEXA scanning and boning. This meant that beef sides were chilled for 1 to 3 days prior to DEXA scanning and boning out, depending on carcase availability. The right side of carcasses were DEXA scanned at abattoir line speed. X-ray images were generated using a single emission from a 140 kV and 27 mA X-ray tube, with a set of 2 images captured on a detector comprised of 2 photodiodes separated by a copper filter (Scott Automation and Robotics). ZnSe was used as a scintillant in the first photodiode, and CsI was used as a scintillant in the second. These scintillants were selected due to their specificity for low and high energy photons respectively (Ryzhikov et al.). To capture the entire beef carcase side this apparatus was duplicated vertically, with the upper being trained on the hindquarter of the beef side and the lower trained on the forequarter. Thus, every time a beef side was scanned a set of 2 images of the forequarter (low and high energy) and 2 images of the hindquarter (low and high energy) were captured. Following DEXA scanning, beef sides were boned out on the same day.

**Figure 1.** A schematic diagram showing duplication of DEXA apparatus' vertically to ensure entire beef sides are scanned simultaneously. This involves one DEXA apparatus scanning the forequarter and another the hindquarter.



### 2.3 Bone-out protocol and lean trim measurement

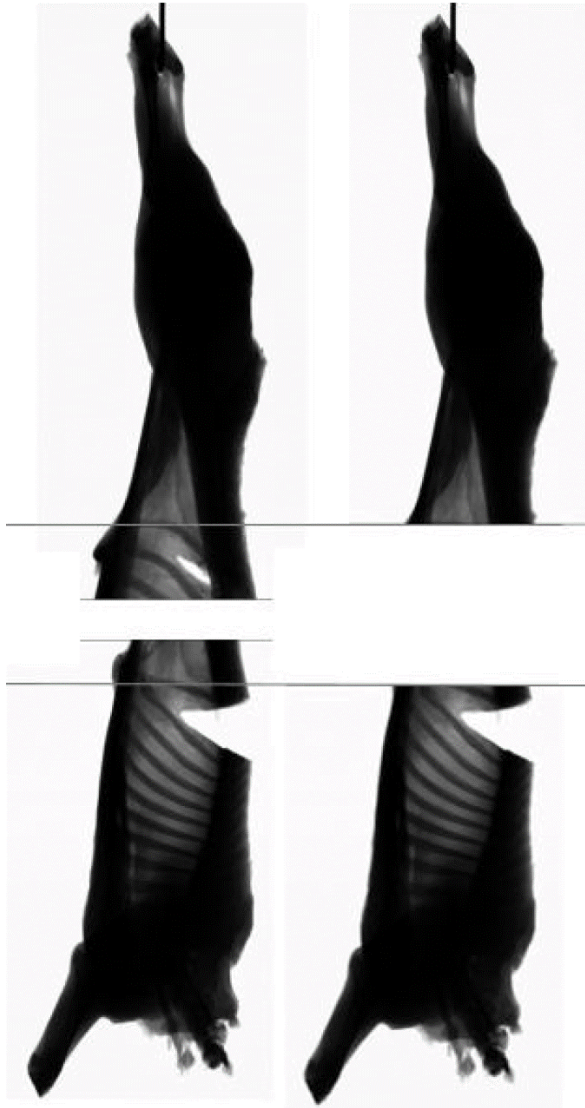
A specialist Teys boner procured all the cuts and trim from beef carcasses, ensuring the same detailed protocol was followed for each side. Beef sides were first boned out to AUSMEAT primal cut specifications and then trimmed to 6mm fat cover using an established protocol based on Teys sub-primal cut specifications. The lean trim procured from each side was differentiated visually by the boner into one of three categories: 65%, 85% or 90% chemical lean (CL) trim, according to standard Teys commercial practice. The actual chemical lean of this trim was not measured. The weight of each trim category was recorded for each individual cut and summed for each side, while cuts and their associated trim were also attributed to either the forequarter (FQ) or hindquarter (HQ) and summed to produce FQ and HQ trim weights. At each step of the bone-out, weights of the commercial cuts, bone, lean trim and fat trim were reconciled against the original primal weight from which they were dissected, to ensure there was full recovery of the original weight and thereby reduce any dissection errors.

### 2.4 DEXA image analysis

Prior to analysis all DEXA images were cropped and calibrated. As upper and lower DEXA images overlap by approximately 30cm (Figure 2), a midsection of the beef sides was captured in both images. However, the portion of each beef side duplicated depends on the length of the carcass. To remove the duplicated section from DEXA images, upper and lower images were cropped at an anatomical landmark, the caudal aspect of the 13<sup>th</sup> rib, as demonstrated in Figure 2.

**Figure 2.** An example of image cropping at the level of the caudal aspect of the 13<sup>th</sup> rib applied to all DEXA images.

Original DEXA Images	Cropped DEXA Images
-------------------------	------------------------



All DEXA images were then calibrated by scaling the pixels corresponding to un-attenuated regions (scans of air) to a value of 4095. R-values were then calculated for each pixel in DEXA images, that is a ratio of photon attenuation between corresponding low and high energy pixels (Pietrobelli et al., 1996), according to the following established formula:

$$(R = \ln(I_{\text{Low}}/\text{AirAtten}) / \ln(I_{\text{High}}/\text{AirAtten}));$$

Where:  $I_{\text{Low}}$  represents the pixel value in the low energy image (ZnSe Photodiode)

$I_{\text{High}}$  represents the pixel value in the high energy image (CsI Photodiode)

AirAtten represents the pixel value corresponding to the un-attenuated photons within each image that have passed through air only (adjusted to 4095).

The average R-value for all pixels in the carcass side image was then calculated and used as a threshold to delete predominately bone-containing pixels. While there are imperfections to this step (Gardner et al., 2015), the objective was to produce a final image consisting of predominately fat and lean tissue. Prior DEXA scanning of tissue phantoms of varying fat



composition (from 100% lean:0% fat to 0% lean:100% fat), and varying thickness (from 12.5 to 280mm thick) then allowed the R values of all soft tissue pixels to be converted to a chemical value and weighted by their estimated tissue thickness. The mean of these pixel values was calculated, and the percentage value subtracted from 100 to derive a “DEXA value” representing carcass lean.

A further two image-components were derived from DEXA images: average Ln(pixel value) indicating carcass thickness and total pixel count, indicating image area/carcass cross-sectional area. The low energy images can be used to determine thickness by taking the average of all logged pixel values in the low energy image (average Ln(pixel value)) after the above thresholding has been applied (Gardner et al., 2015). The pixels in images produced by the DEXA system at Teys Lakes Creek have consistent dimensions, thus image area can be calculated by summation of all pixels in the image prior to the bone thresholding step (Total Pixel Count). As upper and lower images were analysed separately, two DEXA values, total pixel counts and average Ln(pixel values) were calculated for each side, producing a total of 6 DEXA image variables per beef side scanned.

## 2.5 Statistical Analysis

Thirteen carcasses were excluded from the study for >2kg difference in HSW between the left and right sides. This discrepancy occurs when carcasses are not accurately split down the midline, referred to as ‘soft siding’.

### 2.5.1 Data transformation and adjustment

Conversion of lean trim weights and HSW to natural logarithms enabled the use of Huxley’s allometric equation ( $y = ax^b$ ) in this analysis. The equation is structured such that  $x$  is the independent variable,  $a$  is the proportionality co-efficient and  $b$  is the growth coefficient of  $y$  relative to  $x$  (Huxley & Teissier, 1936). Transformation of trim weight and HSW to natural logarithms ensures that the data is linearised ( $\log_e y = \log_e a + b \log_e x$ ) and can then be solved using least squares regression, where  $\log_e$  trim weight ( $y$ ) is predicted by  $\log_e$  HSW ( $x$ ). For our analysis, the use of a logarithmic equation carries three key advantages. Firstly, it allows the maturation rate for each trim weight category to be interpreted. The  $b$  coefficient represents the growth rate of variable ( $y$ ) relative to HSW and will be either: early maturing ( $b < 1$ ), late maturing ( $b > 1$ ) or maturing at the same rate as variable  $x$  ( $b = 1$ ). Secondly, growth data variance increases with scale displaying heteroskedasticity. This variance can be homogenised across the entire data range through logarithmic transformation of the equation. Finally, the natural logarithm format of the equation enables for direct comparison in the differences between  $\log_e y$  values as a percentage difference in trim weight (Cole, 2000), and it is based on this premise that the data presented in this paper has been interpreted.

### 2.5.2 Linear modelling to predict cut weights from DEXA

Initially, multivariate ANOVA models (MANOVA) were used in SAS (SAS version 9.0, SAS Institute, Cary, NC, USA) to test the ability of HSW and P8 fat or DEXA variables to predict 65, 85 and 90% trim weights from the forequarter, hindquarter, or entire beef side. Given the anticipated difficulty of the boner to accurately differentiate 85% from 90% lean trim, these trim weights were summed into a single value (85+90%) and predicted in a second multivariate

model with 65% trim values. Multivariate models were used to account for any associations between trim categories.

Three prediction models were tested for their ability to predict the different trim categories:

- 1)  $\log_e$  hot side weight + P8 fat
- 2)  $\log_e$  hot side weight + DEXA values (upper + lower image)
- 3)  $\log_e$  hot side weight + DEXA values (upper + lower image) + image-components (total pixel count and average  $\ln(\text{pixel value})$  of upper + lower image)

All MANOVA models were initially run with quadratic terms for each independent variable, ensuring that any curvilinear associations between terms were accounted for. All non-significant terms ( $P > 0.05$ ) in multivariate models were removed to ensure the significance and coefficient values of remaining variables were unchanged. This step enabled us to establish a uniform model for each of the dependent variables, and to determine the partial correlation between the dependant variables adjusted for the terms in the model.

Generalised linear models retaining all independent terms from corresponding multivariate models were then used to test the ability of HSW and P8 fat or DEXA variables to predict the weight of each trim category. The three different predictors were tested for their ability to predict the lean trim weight produced from the FQ, HQ or entire beef side based on both original multivariate models (65%, 85% and 90%, or 65% and 85+90%).

The R-squared ( $R^2$ ) and root mean square error (RMSE) were reported to demonstrate the precision with which different models predicted trim weights. The ability of each prediction model to differentiate trim weight variation at a given beef side weight was also shown. To do this each model was used to predict  $\log_e$  trim weight ( $y$ ) of each carcass side and then this predicted value was regressed against  $\log_e$  HSW ( $x$ ). The RMSE of this relationship represented the capacity of the fatness indicator to differentiate the mass of the trim as a percentage difference of the trim weight. Four times the RMSE value ( $\text{mean} \pm 2 \times \text{RMSE}$ ) represents 95% of the trim weight range differentiated by the model, and was reported for carcass sides of 90kg, 160kg and 230kg in weight. These side weights are used as they represent the upper, lower and midpoint of carcass side weights in this study.

Lastly, to assess the robustness of prediction models a 5-fold cross validation was performed. Data was randomly divided into 5 equal groups, balanced for HSW and P8 fat depth. For each trim category, the associated prediction model was trained in 80% of the data (4 groups) and validated in the remaining 20% of the data (1 group). The process was repeated 5 times in total, with each model being validated in each of the 5 groups of data separately, meaning 100% of the data had been used to cross validate the prediction equation. For the relationship between actual versus predicted  $\log_e$  trim weights,  $R^2$  and root mean square error of the prediction (RMSEP) of the five validation tests were averaged, indicating the precision of each of the prediction models. Mean, standard deviation, minimum and maximum of the  $R^2$  and RMSEP values from the 5 validation tests were also reported.

Accuracy of the relationship between actual vs predicted values is demonstrated by the bias and slope. The bias represents the difference between predicted and actual values at the mean of the dataset. Slope represents the deviation of the slope of the relationship from 1 and demonstrates that bias may differ for trim weights lying above or below the mean. The

mean and standard deviation of absolute bias and slope values are reported, as well as the minimum and maximum values across the 5 validation tests.

### 3 Results

The descriptive beef carcass statistics demonstrating the range in carcass side weight, P8 fat depth and trim weights are shown in Table 1.

**Table 1.** Mean  $\pm$  standard deviation (minimum, maximum) of hot carcass side weight, P8 fat and the weight of each trim produced from the whole side (Total), forequarter (FQ) and hindquarter (HQ). These descriptive stats are also shown for each of the 5 subsets of data used to validate of prediction models.

Variable	All Data		Validation Data subsets			
	N=250	Subset 1 (N=50)	Subset 2 (N=50)	Subset 3 (N=50)	Subset 4 (N=50)	Subset 5 (N=50)
Hot side Weight (kg)	144.96 $\pm$ 26.7 7 (235.5,89.5)	144.96 $\pm$ 27.9 9 (235.5,89.5)	144.87 $\pm$ 26.7 (215,98)	144.62 $\pm$ 26.4 6 (207,98.5)	144.82 $\pm$ 26.7 (211.5,98.5)	144.89 $\pm$ 27.0 4 (221,94)
P8 fat depth (mm)	11.44 $\pm$ 4.65 (32,3)	11.44 $\pm$ 4.04 (23,5)	11.76 $\pm$ 4.32 (24,3)	12.5 $\pm$ 4.52 (31,4)	11.74 $\pm$ 5.27 (28,3)	12.84 $\pm$ 5.01 (32,3)
Total 65CL (kg)	10.15 $\pm$ 2.31 (18.26,5.43)	10.15 $\pm$ 2.24 (16.5,5.63)	10.06 $\pm$ 2.18 (15.17,5.59)	10.31 $\pm$ 2.38 (15.81,5.93)	9.93 $\pm$ 2.36 (16.43,5.43)	10.21 $\pm$ 2.46 (18.26,5.96)
Total 85CL (kg)	9.29 $\pm$ 2.49 (21.16,3.87)	9.29 $\pm$ 2.37 (17.8,5.46)	9.1 $\pm$ 2.38 (16.16,5.4)	9 $\pm$ 2.75 (16.66,3.87)	9.01 $\pm$ 2.27 (14.41,4.93)	9.5 $\pm$ 2.7 (21.16,4.82)
Total 90CL (kg)	10.95 $\pm$ 2.58 (20.89,3.76)	10.95 $\pm$ 2.78 (20.89,6.43)	10.57 $\pm$ 2.63 (17.94,3.76)	10.54 $\pm$ 2.08 (16.48,6.07)	10.83 $\pm$ 2.93 (17.87,4.5)	10.39 $\pm$ 2.47 (15.28,5.58)
FQ 65CL (kg)	5.04 $\pm$ 1.47 (10.04,2.1)	5.04 $\pm$ 1.38 (9.07,2.35)	5.1 $\pm$ 1.39 (8.63,2.17)	5.41 $\pm$ 1.53 (9.14,2.9)	5.02 $\pm$ 1.44 (8.8,2.79)	5.21 $\pm$ 1.61 (10.04,2.1)
FQ 85CL (kg)	8.26 $\pm$ 2.38 (19.15,3.25)	8.26 $\pm$ 2.14 (14.91,4.81)	7.98 $\pm$ 2.29 (15.06,4.05)	8 $\pm$ 2.76 (16.19,3.25)	8.02 $\pm$ 2.1 (12.75,4.64)	8.48 $\pm$ 2.61 (19.15,4.27)
FQ 90CL (kg)	8.74 $\pm$ 2.27 (17.59,1.92)	8.74 $\pm$ 2.38 (17.59,4.98)	8.37 $\pm$ 2.31 (14.84,1.92)	8.38 $\pm$ 1.83 (13.76,4.46)	8.55 $\pm$ 2.66 (15.09,3.02)	8.19 $\pm$ 2.12 (12.69,4.13)
HQ 65CL (kg)	5.11 $\pm$ 1 (8.22,2.65)	5.11 $\pm$ 0.96 (7.43,2.98)	4.96 $\pm$ 0.97 (7.69,3.28)	4.9 $\pm$ 1.02 (7.07,2.69)	4.91 $\pm$ 1.03 (7.65,2.65)	5 $\pm$ 1.06 (8.22,3.27)
HQ 85CL (kg)	1.03 $\pm$ 0.47 (2.89,0.12)	1.03 $\pm$ 0.5 (2.89,0.31)	1.12 $\pm$ 0.52 (2.85,0.25)	0.99 $\pm$ 0.4 (2.7,0.38)	0.99 $\pm$ 0.46 (2.69,0.12)	1.02 $\pm$ 0.48 (2.38,0.3)
HQ 90CL (kg)	2.21 $\pm$ 0.46 (3.8,1.35)	2.21 $\pm$ 0.5 (3.3,1.45)	2.21 $\pm$ 0.49 (3.42,1.35)	2.16 $\pm$ 0.44 (3.8,1.42)	2.27 $\pm$ 0.45 (3.59,1.48)	2.21 $\pm$ 0.44 (3.05,1.46)

The correlations between DEXA variables are shown in Table 2. The DEXA Value, Image Area and Image Thickness variables from the upper image were highly correlated with the corresponding measure in the lower DEXA image (Table 2). There was a strong negative correlation for the Image Area and Image Thickness variables in both the upper and lower images (-0.68 and -0.83), while image DEXA Value was poorly correlated (<0.1) to both image area and thickness variables in both upper and lower images (Table 2).

**Table 2.** Simple correlations between hot side weight (HSW), and DEXA value, image area, and image thickness for the lower (fore) and upper (hind section) of beef DEXA images.

HSW	Ln (HSW)	Lower Image Area	Lower Image Thickness	Lower DEXA Value	Upper Image Area	Upper Image Thickness	Upper DEXA Value

HSW	1	0.993	0.829	-0.892	-0.073*	0.703	-0.664	-0.371
Ln (HSW)		1	0.835	-0.889	-0.071*	0.710	-0.675	-0.384
Lower Image Area			1	-0.833	0.056*	0.759	-0.532	-0.202
Lower Image Thickness				1	-0.032*	-0.713	0.794	0.325
Lower DEXA Value					1	0.097*	-0.110*	0.679
Upper Image Area						1	-0.683	-0.309
Upper Image Thickness							1	0.286
Upper DEXA Value								1

\*, P > 0.05

Models predicting total beef side trim weight were moderately precise. 65% CL trim was predicted with greater precision ( $R^2$  of 0.77-0.78 and RMSE of 106-107g) than 90% CL ( $R^2$  of 0.64-0.70 and RMSE of 152-700g) or 85% CL ( $R^2$  of 0.58-0.64 and RMSE of 156-600g) (Table 3). The best precision of side trim weight was demonstrated when lean trim categories were combined, with 85+90% trim predicted with  $R^2$  of 0.90-0.91 and RMSE of only 61-65g (Table 3). FQ trim weights were predicted with very similar precision to trim produced from the entire beef sides (Table 4), however the precision of prediction models were markedly reduced when predicting trim weights procured from the HQ (Table 5). 85% trim was consistently predicted with the lowest precision while combined 85+90% trim was consistently predicted with the highest precision (Tables 3-5).

Using DEXA values as carcass fatness indicators improved the precision of trim weight predictions compared to P8 fat depth, though by only a small amount (Tables 3, 4 and 5). The improved precision of DEXA value models resulted in the ability to differentiate a greater range in lean trim weight than P8 fat models. At an average side weight of 160kg, the DEXA value model could differentiate 1432g of 85+90% lean trim between different carcasses of the same weight, 507g greater than the mass differentiated by P8 fat models (Table 3). Inclusion of DEXA image-components along with DEXA values in prediction models produced the most precise predictions of lean trim (Table 3). DEXA image-component models predicted 85+90% lean trim with an R-squared of 0.91 and a RMSE of 61g and were able to differentiate up to 1794g difference in lean trim weight from sides weighing 160kg, 869g greater than differentiated by P8 fat models (Table 3).

The improved precision of DEXA values and particularly DEXA image-component models over P8 fat prediction models was consistent when predicting the trim produced from only the forequarter of beef sides (Table 4). However, in the less precise hindquarter trim predictions,

P8 fat prediction models were marginally more precise than DEXA image-component models when predicting 65% and 85% CL trim weights (Table 5).

**Table 3.** Models predicting entire beef side lean trim weights including F-values, coefficient, intercept, coefficient of determination (R<sup>2</sup>), and root mean square error (RMSE), as well as the difference in trim weights that can be seen by each model at hot carcass side weight (HSW) of 90, 160 and 230 kg.

	MANOVA Model 1			MANOVA Model 2	
	Ln (Total 65CL)	Ln (Total 85CL)	Ln (Total 90CL)	Ln (Total 65CL)	Ln (Total 85+90CL)
<b>P8 Models</b>					
	<i>F-Values</i>				
Ln (HSW)	678**	306**	431**	678**	2141**
P8 Tissue Depth (mm)	19.4**	1.6	15.7**	19.4**	11.5**
	<i>Coefficients</i>				
Intercept	-2.83±0.189	-3.03±0.290	-3.17±0.264	-2.83±0.189	-2.36±0.113
Ln (HSW)	1.02±0.0390	1.04±0.0597	1.13±0.0545	1.02±0.0390	1.08±0.0234
P8 Tissue Depth (mm)	0.0068±0.0015	0.0029±0.0024	-0.0085±0.0022	0.0068±0.0015	-0.0031±0.0009
	<i>Difference Estimates</i>				
Differences at 90-160-230kg	0.787-1.020- 1.252	0.252-0.327- 0.401	0.960-1.243- 1.527	0.787-1.020- 1.252	0.714-0.925-1.136
	<i>Precision Indicators</i>				
R <sup>2</sup>	0.77	0.58	0.64	0.77	0.90
RMSE	0.109	0.166	0.152	0.109	0.065
<b>DEXA Models</b>					
	<i>F-Values</i>				
Ln (HSW)	628**	320**	418**	630**	2083**
Lower DEXA value	0.8	6.7*	25.6**	13.3**	5.8*
Upper DEXA value	0.3	3.6	5.8*	0.4	26.8**
	<i>Coefficients</i>				
Intercept	-0.2526±2.83	7.33±4.16	-22.87±3.67	-2.28±0.3191	-3.04±0.1853
Ln (HSW)	1.06±0.0424	1.12±0.0625	1.13±0.0551	1.06±0.0423	1.12±0.0246
Lower DEXA Value	-0.0530±0.0606	-0.2312±0.0892	0.3981±0.0787	-0.0092±0.0025	-0.0035±0.0015
Upper DEXA Value	0.0018±0.0031	0.0085±0.0045	0.0096±0.0040	0.0019±0.0030	0.0091±0.0018
	<i>Difference Estimates</i>				
Differences at 90-160-230kg	0.732-0.948- 1.164	1.062-1.376- 1.690	1.524-1.974- 2.424	0.732-0.948- 1.164	1.106-1.432-1.759
	<i>Precision Indicators</i>				
R <sup>2</sup>	0.77	0.60	0.69	0.77	0.91
RMSE	0.109	0.160	0.141	0.109	0.063
<b>DEXA image-component Models</b>					
	<i>F-Values</i>				
Ln (HSW)	150**	129**	64.8**	150**	528**
Lower DEXA Value	0.4	6.0*	21.5**	12.9**	2.8
Lower Image Area	0.8	1.2	0.4	1.1	8.7**
Lower Image Thickness	1.1	6.3*	0.0	1.1	12.8**
Upper DEXA Value	1.4	2.5	3.2	1.4	19.6**
Upper Image Area	-	-	-	-	-
Upper Image Thickness	-	-	-	-	-
	<i>Coefficients</i>				
Intercept	-11.31±10.66	41.63±15.49	-20.27±13.86	-12.91±10.13	16.53±5.76
Ln (HSW)	1.14±0.0935	1.55±0.1359	0.9792±0.1216	1.14±0.0934	1.22±0.0531
Lower DEXA Value	-0.0403±0.0623	-0.2215±0.0906	0.3757±0.0810	-0.0097±0.0027	-0.0026±0.0015
Lower Image Area	-3.8E-6±4.24E-6	6.9E-6±6.17E-6	3.7E-6±5.52E-6	-4.3E-6±4.12E-6	6.9E-6±2.34E-6
Lower Image Thickness	3.02±2.92	-10.67±4.24	-0.4503±3.79	3.08±2.91	-5.92±1.65
Upper DEXA Value	0.0039±0.0033	0.0075±0.0048	0.0076±0.0043	0.0039±0.0033	0.0082±0.0019
Upper Image Area	-	-	-	-	-
Upper Image Thickness	-	-	-	-	-
	<i>Difference Estimates</i>				
Differences at 90-160-230kg	0.850-1.100- 1.351	1.365-1.768- 2.172	1.631-2.113- 2.594	0.867-1.123- 1.379	1.385-1.794-2.203
	<i>Precision Indicators</i>				
R <sup>2</sup>	0.78	0.64	0.70	0.78	0.91
RMSE	0.107	0.156	0.140	0.107	0.061

\*, P<0.05; \*\*,P<0.01.

**Table 4.** Models predicting forequarter trim weights including F-values, coefficient, intercept, coefficient of determination (R<sup>2</sup>), and root mean square error (RMSE), as well as the difference in trim weights that can be seen by each model at hot carcass side weight (HSW) of 90, 160 and 230 kg.

	MANOVA Model 1			MANOVA Model 2	
	Ln (FQ 65CL)	Ln (FQ 85CL)	Ln (FQ 90CL)	Ln (FQ 65CL)	Ln (FQ 85+90CL)
<b>P8 Models</b>					
	<i>F-Values</i>				
Ln (HSW)	618**	220**	300**	618**	1583**
P8 Tissue Depth (mm)	14.1**	3.4	10.4**	14.1**	3.3
	<i>Coefficients</i>				
Intercept	-4.73±0.246	-3.11±0.337	-3.77±0.338	-4.73±0.246	-2.67±0.135
Ln (HSW)	1.26±0.0507	1.03±0.0695	1.20±0.0696	1.26±0.0507	1.10±0.0278
P8 Tissue Depth (mm)	0.0075±0.0020	0.0051±0.0027	-0.0089±0.0028	0.0075±0.0020	-0.0020±0.0011
	<i>Difference Estimates</i>				
Differences at 90-160-230kg	0.449-0.582- 0.714	0.449-0.581- 0.714	0.788-1.021- 1.254	0.449-0.582- 0.714	0.364-0.472- 0.579
	<i>Precision Indicators</i>				
R <sup>2</sup>	0.75	0.51	0.55	0.75	0.87
RMSE	0.141	0.194	0.194	0.141	0.077
<b>DEXA Models</b>					
	<i>F-Values</i>				
Ln (HSW)	585**	251**	285**	589**	1637**
Lower DEXA Value	0.3	8.9**	27.8**	16.5**	14.8**
Upper DEXA Value	0.0	5.2*	4.3*	0.0	29.6**
	<i>Coefficients</i>				
Intercept	-2.37±3.56	10.58±4.79	-29.79±4.71	-3.66±0.4023	-3.32±0.2168
Ln (HSW)	1.30±0.0536	1.14±0.0720	1.20±0.0708	1.29±0.0533	1.16±0.0287
Lower DEXA Value	-0.0407±0.0765	-0.3075±0.1029	0.5330±0.1011	-0.0129±0.0032	-0.0066±0.0017
Upper DEXA Value	3.8x10 <sup>-4</sup> ±0.0038	0.0118±0.0052	0.0106±0.0051	4.6x10 <sup>-4</sup> ±0.0038	0.0112±0.0021
	<i>Difference Estimates</i>				
Differences at 90-160-230kg	0.782-1.013- 1.244	1.394-1.806- 2.217	1.478-1.914- 2.350	0.783-1.014- 1.245	1.555-2.015- 2.474
	<i>Precision Indicators</i>				
R <sup>2</sup>	0.77	0.56	0.61	0.77	0.88
RMSE	0.137	0.184	0.181	0.137	0.074
<b>DEXA image-component Models</b>					
	<i>F-Values</i>				
Ln (HSW)	119**	97.9**	41.3**	121**	401**
Lower DEXA Value	0.2	6.8**	25.5**	17.0**	6.7*
Lower Image Area	9.5**	1.7	6.5*	4.4*	6.9**
Lower Image Thickness	0.8	4.3*	0.0	5.7*	10.6**
Upper DEXA Value	1.2	3.1	2.4	0.4	20.3**
Upper Image Area	-	-	-	-	-
Upper Image Thickness	-	-	-	4.6*	2.2
	<i>Coefficients</i>				
Intercept	-10.70±10.72	35.85±14.43	-30.66±14.32	118.76±66.30	-36.55±35.51
Ln (HSW)	1.27±0.1165	1.55±0.1569	1.00±0.1557	1.29±0.1168	1.25±0.0625
Lower DEXA Value	-0.0349±0.0758	-0.2657±0.1021	0.5119±0.1014	-0.0142±0.0034	-0.0048±0.0018
Lower Image Area	-2.2x10 <sup>-6</sup> ± 7.2x10 <sup>-7</sup>	-1.3x10 <sup>-6</sup> ± 9.7x10 <sup>-7</sup>	2.4x10 <sup>-6</sup> ± 9.6x10 <sup>-7</sup>	-1.1x10 <sup>-5</sup> ± 5.4x10 <sup>-6</sup>	7.6x10 <sup>-6</sup> ± 2.9x10 <sup>-6</sup>
Lower Image Thickness	2.63±2.96	-8.30±3.99	0.6047±3.95	10.74±4.51	-7.89±2.42
Upper DEXA Value	0.0044±0.0040	0.0095±0.0054	0.0083±0.0053	0.0027±0.0041	0.0099±0.0022
Upper Image Area	-	-	-	-	-
Upper Image Thickness	-	-	-	-42.46±19.89	15.86±10.66
	<i>Difference Estimates</i>				
Differences at 90-160-230kg	0.747-0.968- 1.188	1.553-2.011- 2.469	1.513-1.959- 2.406	0.747-0.968- 1.188	1.463-1.894- 2.326
	<i>Precision Indicators</i>				
R <sup>2</sup>	0.78	0.58	0.62	0.78	0.89
RMSE	0.135	0.181	0.180	0.133	0.071

\*, P<0.05; \*\*, P<0.01.

**Table 5.** Models predicting hindquarter trim weights including F-values, coefficient, intercept, coefficient of determination (R<sup>2</sup>), and root mean square error (RMSE), as well as the difference in trim weights that can be seen by each model at hot carcass side weight (HSW) of 90, 160 and 230 kg.

	MANOVA Model 1			MANOVA Model 2	
	Ln (HQ 65CL)	Ln (HQ 85CL)	Ln (HQ 90CL)	Ln (HQ 65CL)	Ln (HQ 85+90CL)
<b>P8 Models</b>					
			<i>F-Values</i>		
Ln (HSW)	244**	54.9**	333**	244**	377**
P8 Tissue Depth (mm)	10.4**	6.3*	10.6**	10.4**	18.4**
			<i>Coefficients</i>		
Intercept	-2.29±0.24	-5.41±0.73	-3.55±0.24	-2.29±0.24	-3.47±0.24
Ln (HSW)	0.77±0.0490	1.11±0.15	0.89±0.0485	0.77±0.0490	0.95±0.0490
P8 Tissue Depth (mm)	0.0062±0.0019	-0.0149±0.0059	-0.0063±0.0019	0.0062±0.0019	-0.0083±0.0019
			<i>Difference Estimates</i>		
Differences at 90-160-230kg	0.332-0.430-0.528	0.148-0.191-0.235	0.145-0.188-0.231	0.332-0.430-0.528	0.281-0.364-0.447
			<i>Precision Indicators</i>		
R <sup>2</sup>	0.55	0.18	0.58	0.55	0.61
RMSE	0.136	0.418	0.135	0.136	0.137
<b>DEXA Models</b>					
			<i>F-Values</i>		
Ln (HSW)	279**	50.3**	351**	279**	383**
Lower DEXA Value	2.6	4.2*	22.4**	2.6	26.1**
Upper DEXA Value	-	-	-	-	-
			<i>Coefficients</i>		
Intercept	-2.05±0.33	-6.51±1.00	-4.44±0.31	-2.05±0.33	-4.42±0.32
Ln (HSW)	0.80±0.0480	1.03±0.15	0.86±0.0458	0.80±0.0480	0.91±0.0467
Lower DEXA Value	-0.0037±0.0023	0.0141±0.0069	0.0102±0.0022	-0.0037±0.0023	0.0113±0.0022
Upper DEXA Value	-	-	-	-	-
			<i>Difference Estimates</i>		
Differences at 90-160-230kg	0.159-0.206-0.253	0.117-0.151-0.185	0.197-0.255-0.313	0.159-0.206-0.253	0.315-0.408-0.501
			<i>Precision Indicators</i>		
R <sup>2</sup>	0.54	0.18	0.60	0.54	0.62
RMSE	0.139	0.420	0.132	0.139	0.135
<b>DEXA image-component Models</b>					
			<i>F-Values</i>		
Ln (HSW)	77.8**	10.7**	58.1**	73.8**	74.5**
Lower DEXA value	0.4	3.5	18.7**	0.2	21.4**
Lower Image Area	0.0	0.0	1.7	0.0	2.2
Lower Image Thickness	0.3	1.4	1.7	0.5	3.1
Upper DEXA Value	-	-	-	-	-
Upper Image Area	-	-	-	5.1*	5.2*
Upper Image Thickness	0.1	1.6	0.9	2.9	1.2
			<i>Coefficients</i>		
Intercept	-3.53±1.67	-5.41±5.12	-5.02±1.59	-111.06±62.75	60.73±60.77
Ln (HSW)	1.06±0.120	1.20±0.368	0.875±0.115	1.04±0.121	1.01±0.117
Lower DEXA Value	-0.0015±0.0025	0.014±0.0076	0.010±0.0024	-0.0012±0.0024	0.011±0.0024
Lower Image Area	-5.8x10 <sup>-7</sup> ±4.1x10 <sup>-6</sup>	1.3x10 <sup>-6</sup> ±1.3x10 <sup>-5</sup>	5.1x10 <sup>-6</sup> ±3.9x10 <sup>-6</sup>	-8.6x10 <sup>-7</sup> ±4.1x10 <sup>-6</sup>	5.8x10 <sup>-6</sup> ±3.9x10 <sup>-6</sup>
Lower Image Thickness	0.077±0.143	0.523±0.440	0.178±0.137	0.111±0.151	0.259±0.146
Upper DEXA Value	-	-	-	-	-
Upper Image Area	-	-	-	-2.8x10 <sup>-6</sup> ±1.2x10 <sup>-6</sup>	2.7x10 <sup>-6</sup> ±1.2x10 <sup>-6</sup>
Upper Image Thickness	-0.056±0.209	-0.804±0.641	-0.192±0.199	28.91±16.84	-18.16±16.31
			<i>Difference Estimates</i>		
Differences at 90-160-230kg	0.315-0.408-0.501	0.153-0.198-0.244	0.230-0.297-0.365	0.395-0.511-0.627	0.406-0.526-0.646
			<i>Precision Indicators</i>		
R <sup>2</sup>	0.55	0.18	0.61	0.57	0.64
RMSE	0.138	0.422	0.131	0.136	0.132

\*, P<0.05; \*\*,P<0.01.



Trim weight prediction models (Tables 3, 4 and 5) maintained their precision when cross validated (Table 6). Given that the combined lean trims (85+90% CL) was predicted with far greater precision than 85 or 90% CL separately, the validation of 65% and 85+90% CL are shown (Table 6). These validation tests demonstrated that the predictions had good accuracy, with absolute bias values close to zero, and the slopes of the relationships between actual and predicted values very close to 1 (Table 6).

**Table 6** Precision and accuracy estimates of leave-one-out cross validation models predicting lean trim weights from hot side weight (kg) and P8 fat, DEXA value, or DEXA-image-components in the entire beef side (TOTAL), forequarter (FQ) and hindquarter (HQ). Precision estimates include R-squared ( $R^2$ ) and root mean square error of prediction (RMSEP). Accuracy estimates include absolute slope from 1 (Slope), representing the relationship between actual and predicted values, and absolute bias (Bias) which represents the difference between actual minus predicted values at the mean of the dataset. Each prediction model was validated within 5 data sets, with the mean, standard deviation, minimum and maximum of those 5 tests reported. RMSEP and bias values can be interpreted as a proportion of the weight of the trim.

		P8 value	DEXA Value	DEXA image-components
TOTAL 65CL	$R^2$	0.773±0.04 (0.74,0.84)	0.775±0.04 (0.74,0.84)	0.783±0.04 (0.75,0.84)
	RMSEP	0.109±0.013 (0.09,0.12)	0.108±0.012 (0.09,0.12)	0.106±0.012 (0.09,0.12)
	Slope	0.000±0.029 (0.98,1.05)	0.001±0.047 (0.96,1.07)	0.000±0.032 (0.97,1.05)
	Bias	0.010±0.007 (-0.02,0.01)	0.008±0.006 (-0.02,0.01)	0.009±0.005 (-0.02,0.01)
TOTAL 85+90CL	$R^2$	0.905±0.02 (0.89,0.92)	0.911±0.02 (0.89,0.93)	0.917±0.01 (0.91,0.94)
	RMSEP	0.064±0.008 (0.06,0.08)	0.062±0.009 (0.05,0.07)	0.060±0.006 (0.05,0.07)
	Slope	0.000±0.049 (0.94,1.05)	0.000±0.049 (0.94,1.04)	0.000±0.051 (0.93,1.06)
	Bias	0.009±0.005 (-0.01,0.02)	0.006±0.005 (-0.01,0.01)	0.005±0.006 (-0.01,0.01)
FQ 65CL	$R^2$	0.750±0.07 (0.63,0.81)	0.761±0.08 (0.64,0.85)	0.774±0.07 (0.66,0.85)
	RMSEP	0.142±0.027 (0.12,0.19)	0.138±0.030 (0.11,0.18)	0.135±0.028 (0.11,0.18)
	Slope	0.001±0.029 (0.97,1.04)	0.000±0.036 (0.97,1.06)	0.001±0.034 (0.96,1.04)
	Bias	0.019±0.017 (-0.02,0.05)	0.017±0.013 (-0.02,0.04)	0.017±0.011 (-0.02,0.03)
FQ 85+90CL	$R^2$	0.874±0.03 (0.85,0.92)	0.875±0.02 (0.86,0.92)	0.887±0.02 (0.87,0.93)
	RMSEP	0.077±0.008 (0.06,0.08)	0.077±0.007 (0.06,0.08)	0.073±0.009 (0.06,0.08)
	Slope	0.000±0.045 (0.94,1.06)	0.000±0.048 (0.94,1.06)	0.000±0.048 (0.93,1.05)
	Bias	0.011±0.007 (-0.01,0.02)	0.008±0.007 (-0.01,0.02)	0.007±0.008 (-0.01,0.02)
HQ 65CL	$R^2$	0.553±0.09 (0.42,0.66)	0.561±0.07 (0.45,0.65)	0.547±0.08 (0.43,0.65)
	RMSEP	0.137±0.014 (0.11,0.15)	0.136±0.013 (0.12,0.15)	0.138±0.014 (0.11,0.15)
	Slope	0.000±0.103 (0.84,1.11)	0.000±0.086 (0.87,1.11)	0.002±0.112 (0.83,1.13)
	Bias	0.014±0.013 (-0.02,0.03)	0.014±0.012 (-0.02,0.03)	0.015±0.009 (-0.02,0.03)
HQ 85+90CL	$R^2$	0.579±0.12 (0.40,0.73)	0.608±0.11 (0.43,0.74)	0.619±0.11 (0.46,0.75)
	RMSEP	0.141±0.015 (0.12,0.15)	0.136±0.014 (0.12,0.15)	0.134±0.013 (0.11,0.15)
	Slope	0.003±0.146 (0.76,1.13)	0.002±0.135 (0.76,1.10)	0.000±0.143 (0.77,1.12)
	Bias	0.010±0.007 (-0.02,0.02)	0.006±0.006 (-0.01,0.02)	0.007±0.007 (-0.01,0.02)

NB: The mean ± SD values reported for bias and slope are calculated using the mean of the absolute values from the 5 validation tests.

## 4 Discussion

### 4.1 Precision and accuracy of DEXA prediction of trim weights

In support of our hypothesis, the results demonstrate that in most cases DEXA variables can predict beef trim weights with higher precision and accuracy than models using the current measure of carcass fatness, P8 fat depth. This difference in prediction power was evident through small differences in precision indicators (R-square and RMSE), but also through the capacity of DEXA models were to discriminate more variation in trim weight at a set carcass weight than models using P8 fat. The extent of these differences varied depending on carcass region, weight, and trim category. DEXA variables differentiated up to 500g more variation in fatter trim (65% CL), while in leaner trim weight (85+90% CL) these differences were even more marked, with DEXA variables differentiating up to 1.9kg more variation compared to P8 fat models. This is likely due to the improved measurement of carcass composition using DEXA, which is able to quantify tissue composition throughout the entire carcass, in contrast to P8 fat depth which relies on the association between a fat depth at a single site with fatness throughout the carcass. This correlation is highly variable, with single-point fatness measures poorly predicting whole beef carcass fatness as measured by the gold standard method medical CT scanning (Williams et al., 2017). In contrast DEXA has been demonstrated to precisely and accurately predict whole carcass composition in a commercial setting, albeit in lamb (Gardner et al., 2017).

The inclusion of DEXA image-components in addition to DEXA values resulted in slight improvements to precision, as indicated by superior R-squared and RMSE values. DEXA image-component models were thus capable of discerning a slightly greater range in trim weight than models containing only DEXA values, and a substantially greater range in trim weight than P8 fat depth models. This suggests that these DEXA image-components are providing additional information on carcass composition than what is captured by the mean DEXA value alone.

Predictions of trim weight procured from the entire side and forequarter were more precise than trim weight predictions from the hindquarter. DEXA image-component models were able to predict leaner trim (85+90% CL) and fatter trim (65% CL) from the forequarter with an R-squared of 0.89 and 0.78. In contrast, DEXA variables were less precise predicting trim from the hindquarter, with R-squared values of 0.64 and 0.57 for leaner and fatter trim respectively. The reduced performance of DEXA image-components in the hindquarter may be due to differences in tissue thickness between fore and hindquarter sections, with the thickest region of a beef side (when scanned in a medial to lateral plane) being the pelvis and upper hind limb. Increasing tissue thickness increases the attenuation of X-rays, particularly in tissues >200mm thick, resulting in a reduced ability of DEXA to differentiate tissue types and precisely measure composition. Additionally, DEXA image-components from lower DEXA images (representing the fore section of each side) accounted for greater variation in trim weight in prediction models than DEXA image-components from the upper or hindquarter images. While more variables from lower DEXA images were retained in models, DEXA variables from the upper image also retained some significance when predicting trim weights, demonstrating some additional composition information is obtained from the upper DEXA images. However, in a commercial setting processors are most likely to use DEXA variables to predict lean trim procured from the entire beef sides, thus the high precision of the models in this scenario is a positive finding for potential commercial applications.

Another key finding of this study was the significant improvement in precision when the leaner trims were summed (85+ 90%) rather than predicted separately. DEXA components models

predicted 85% and 90% CL trim as separate categories with R-squared values of 0.64 and 0.70, yet could predict summed 85+90% lean trim with much higher precision (R-squared of 0.91). These results are likely due to human error in the manually dissected trim weights, rather than deficiency of the DEXA system itself. It is difficult for an operator to visually discriminate between 85% and 90% CL on the boning floor, introducing a certain randomness into which category that operator designates lean trim. The reason that 85% CL was consistently predicted with the less precision than 90% CL is unclear, but likely also related to the subjectivity with which trim is designated to these categories. This finding suggests that processors may need to reassess their justification for differentiating lean trims into 85 and 90% CL categories during fabrication.

Testing the DEXA models using a leave-one-group-out cross validation demonstrated that all models maintained precision upon validation, and that predictions were highly accurate. Minimal differences were seen in R-squared and RMSEP values between trained and validation models, attesting to the stability of these models. This robustness was evident across all models, even those using P8 fat depth. This is likely due to the predictive power of HSW within these models, rather than any fatness indicator. This was clearly demonstrated by the high model F-values for this term, reflecting the fundamental association between component weight and side weight (Berg & Butterfield, 1976). These findings align with another study that utilised sex and 9 characteristic traits to predict lean product, bone, and fat trim yield (Huerta-Leidenz et al., 2018), with carcass weight explaining >90% of the total variation in component weights. This further illustrates the importance of expressing the predictive capacity of these fatness indicators in terms of their ability to differentiate trim weights beyond that already described by carcass weight, as this represents the value of incorporating this additional measure into a processing plant.

## **4.2 Industry implications and future work**

Relatively little work has been published reporting DEXA prediction of carcass composition and cut weights in beef, while no studies have tested the capacity of DEXA to predict beef trim weights. The results of this study support that the commercial beef DEXA system is able to provide an objective measure of carcass composition and thereby predict beef trim weights with better accuracy and precision than the current measure of carcass composition, P8 fatness. It also quantifies the additional mass of trim that can be discriminated by the DEXA system, enabling a clear business case to be established prior to installation of this technology.

These results align with a study by López-Campos et al. (2018) demonstrating that a medical DEXA system can predict beef cut weights with high precision and accuracy, although their work was not undertaken in a commercial setting or at abattoir chain-speed. Alternatively a recent study by Calnan et al. (2021) demonstrated that a prototype rapid DEXA system similar to that used in this study can predict the CT composition of beef carcasses with excellent accuracy and precision. These studies highlight the excellent potential for rapid DEXA scanning to predict beef carcass composition and thereby trim and cut weights commercially in abattoirs. As this trial was conducted using the first rapid DEXA system installed in a beef abattoir globally, the calibration of this system is ongoing. Therefore, the potential also remains to significantly improve trim weight predictions demonstrated in this experiment. Work using plastic calibration blocks representing various percentages of fat and lean are being used to ensure fully calibrate images are produced by the DEXA system, especially when scanning trials are performed across multiple days, such as in this trial. Additionally, while the DEXA

values calculated from images in this trial were based on tissue relationships established by scanning tissue calibration blocks, the DEXA system remains to be fully calibrated against computed tomography (CT), the gold standard measure of carcass composition. Finally, beef DEXA image acquisition provides novel challenges in comparison to lamb due to the differences in hardware requirements for scanning substantially larger beef carcasses, meaning that image analysis techniques are being further developed to ensure optimal beef DEXA variables are produced. As the current beef DEXA system is only in its early stages, the results of this study suggest that DEXA has the potential to be a highly valuable tool to inform pre-fabrication decisions and optimise beef carcass value.

A limitation of the current study was that cattle available for selection were all Bos Indicus cross breeds, cattle commonly produced in Northern Australia. Therefore, while selection was based on side weight and P8 fatness to represent as wide a range as possible in carcass phenotype, further DEXA composition studies need to incorporate Bos taurus cattle to ensure that there is no breed bias and that this technology is applicable across all sectors of the beef industry. Breed effects on DEXA are considered unlikely given the penetrative whole carcass nature of this carcass composition measurement, however future analyses comparing DEXA estimates of carcass composition in Bos indicus and Bos taurus cattle are required to support this assertion.

## 5 Conclusions

This work demonstrates that rapid DEXA can predict lean trim weights of beef sides with greater precision and accuracy than the current industry estimates of carcass composition using P8 fatness. Carcass weight and DEXA variables are able to describe up to 91% of the variation in leaner trim and 78% of the variation in fatter trim weights procured from varied beef sides. The ability to precisely and accurately predict beef trim weights prior to boning out has the potential to strengthen the overall prediction of beef carcass value, which translates to more transparent pricing for producers at the point of sale and the ability for processors to optimise beef products into their highest available markets (Gardner et al., 2021). Future research will report on the ability of an on-line DEXA system to predict beef cut weights in a commercial setting, further quantifying the commercial viability of beef DEXA implementation into beef abattoirs within Australia and the potential returns on investment it will provide to processors and producers alike.

## 6 References

- Berg, R. T., & Butterfield, R. M. (1976). *New concepts of cattle growth*. Sydney U.P.
- Calnan, H., Williams, A., Peterse, J., Starling, S., Cook, J., Connaughton, S., & Gardner, G. E. (2021). A prototype rapid dual energy X-ray absorptiometry (DEXA) system can predict the CT composition of beef carcasses. *Meat science*, 173, 108397. <https://doi.org/https://doi.org/10.1016/j.meatsci.2020.108397>
- Cole, T. J. (2000). Sympercents: Symmetric percentage differences on the 100 log(e) scale simplify the presentation of log transformed data. *Statistics in medicine*, 19(22), 3109-3125. [https://doi.org/10.1002/1097-0258\(20001130\)19:22<3109::AID-SIM558>3.0.CO;2-F](https://doi.org/10.1002/1097-0258(20001130)19:22<3109::AID-SIM558>3.0.CO;2-F)
- Gardner, G., Glendenning, R., Brumby, O., Starling, S., & Williams, A. (2015). The development and calibration of a dual X-ray absorptiometer for estimating carcass composition at abattoir chain-speed. In C. Maltin, C. Craigie, & L. Bunger (Eds.), *Farm Animal Imaging* (pp. 24-26).

- Gardner, G. E., Anderson, F., Smith, C., & Williams, A. (2021). Using dual energy X-ray absorptiometry to estimate commercial cut weights at abattoir chain-speed. *Meat science*, 173, 108400-108400. <https://doi.org/10.1016/j.meatsci.2020.108400>
- Gardner, G. E., Peterse, J., Starling, S. E., Cook, J., Shirazi, M., & Williams, A. (2017). *Developing a dual X-ray absorptiometer for estimating carcass fatness in beef at abattoir chain-speed* International Congress of Meat Science and Technology, Cork, Ireland. [http://icomst-proceedings.helsinki.fi/papers/2017\\_08\\_84.pdf](http://icomst-proceedings.helsinki.fi/papers/2017_08_84.pdf)
- Gardner, G. E., Starling, S., Charnley, J., Hocking-Edwards, J., Peterse, J., & Williams, A. (2018). Calibration of an on-line dual energy X-ray absorptiometer for estimating carcass composition in lamb at abattoir chain-speed. *Meat science*, 144, 91-99. <https://doi.org/https://doi.org/10.1016/j.meatsci.2018.06.020>
- Hocking Edwards, J. E., Smith, C., Gardner, G. E., Pethick, D. W., & Ball, A. J. (2015). *The value of saleable meat yield to lamb processors* International Congress on Meat Science and Technology, Clermont-Ferrand, France.
- Huerta-Leidenz, N., Atencio-Valladares, O., Rodriguez, J., Jerez-Timaure, N., Vargas, G., & Rodas-González, A. (2018). Predictability of lean product, bone, and fat trim in beef carcasses from Costa Rica. *Meat science*, 143, 223-229. <https://doi.org/https://doi.org/10.1016/j.meatsci.2018.05.012>
- Huxley, J. S., & Teissier, G. (1936). Terminology of Relative Growth. *Nature*, 137(3471), 780-781. <https://doi.org/10.1038/137780b0>
- Johnston, D. J., Reverter, A., Burrow, H. M., Oddy, V. H., & Robinson, D. L. (2003). Genetic and phenotypic characterisation of animal, carcass, and meat quality traits from temperate and tropically adapted beef breeds. *Australian Journal of Agricultural Research*, 54(2), 107-118. <https://doi.org/https://doi.org/10.1071/AR02085>
- López-Campos, Ó., Roberts, J. C., Larsen, I. L., Prieto, N., Juárez, M., Dugan, M. E. R., & Aalhus, J. L. (2018). Rapid and non-destructive determination of lean fat and bone content in beef using dual energy X-ray absorptiometry. *Meat science*, 146, 140-146. <https://doi.org/10.1016/j.meatsci.2018.07.009>
- Pietrobelli, A., Formica, C., Wang, Z., & Heymsfield, S. B. (1996). Dual-energy X-ray absorptiometry body composition model: review of physical concepts. *American Journal of Physiology - Endocrinology And Metabolism*, 271(6), 941-951. <https://doi.org/10.1152/ajpendo.1996.271.6.E941>
- Ryzhikov, V. D., Ryzhikov, V. D., Opolonin, A. D., Pashko, P. V., & Svishch, V. M. Instruments and detectors on the base of scintillator crystals ZnSe(Te), CWO, CsI(Tl) for systems of security and customs inspection systems. *Nuclear instruments & methods in physics research. Section A, Accelerators, spectrometers, detectors and associated equipment*, 537(1-2), 424-430. <https://doi.org/10.1016/j.nima.2004.08.056>
- Watson, R., Polkinghorne, R., & Thompson, J. M. (2008). Development of the Meat Standards Australia (MSA) prediction model for beef palatability. *Australian Journal of Experimental Agriculture*, 48(11), 1368-1379. <https://doi.org/https://doi.org/10.1071/EA07184>
- Williams, A., Jose, C., McGilchrist, P., Walmsley, B., McPhee, M., Greenwood, P., & Gardner, G. (2017). *Predicting Beef Carcass Composition from Weight and Rib Fat Depth*.